Manipulation of tunable nonreciprocal entanglement and one-way steering induced by two-photon driving

Si-Yu Guan,[1] Hong-Fu Wang,[1,2,*] and Xuexi Yi[1,†]

[1]*Center for Quantum Sciences and School of Physics, Northeast Normal University, Changchun, Jilin 130024, China*

[2]*Department of Physics, College of Science, Yanbian University, Yanji, Jilin 133002, China*

(Received 31 October 2023; accepted 30 May 2024; published 17 June 2024)

We consider an all-optical system consisting of two whispering-gallery-mode microring resonators and two adjacent optical waveguides. Pumping fields from different directions can simultaneously excite both clockwise and counterclockwise modes in the two resonators. When the propagation direction of the excited photons aligns with the propagation direction of the photons excited by two-photon driving, satisfying the phase-matching conditions, stable nonreciprocal quantum entanglement and one-way Einstein-Podolsky-Rosen (EPR) steering can be effectively generated. This work demonstrates that quantum correlations can only be prepared when the system is driven by a pumping field from the unique port, a condition induced by the nonlinearity of the system. Furthermore, we show that the maximum values of quantum entanglement and one-way EPR steering can be achieved when the frequency detunings of the two optical modes are opposite, and higher two-photon driving strength and coupling strength significantly enhance quantum entanglement and one-way EPR steering. Our study provides a highly manipulable platform, offering promise for one-way quantum computing and quantum communication based on macroscopic entangled states.

DOI: 10.1103/PhysRevA.109.062423

I. INTRODUCTION

Entanglement, serving as a pivotal resource for quantum technologies, plays a fundamental role in quantum computing [1–4], quantum metrology [5,6], and quantum teleportation [7]. It is distinguished by its remarkable capacity to delve into potent nonclassical correlations between disparate quantum systems, even when spatially separated, thus embodying a distinctive hallmark of quantum physics [8]. When entanglement is shared among distinct components within a composite quantum system, it imparts crucial quantum resources for a variety of burgeoning quantum technologies, spanning from quantum information processing [9,10] to quantum sensing [11]. Considerable effort has been dedicated to the generation and control of entanglement [12–16], leading to the progression of quantum-enabled devices beyond their classical counterparts [17]. The concept of Einstein-Podolsky-Rosen (EPR) steering, which represents a refined subset of entanglement, was originally acknowledged by Schrödinger in [18] and subsequently established on a rigorous mathematical basis in Refs. [19,20]. Importantly, in contrast to entanglement and Bell nonlocality [21], the defining characteristic of EPR steering inherently exhibits an asymmetry between two observers [19,22]. Within a bipartite scenario, it encompasses nonclassical correlations where one party can discern the state held by the distant counterpart through local measurements performed on their portion of the entangled state. To date, despite the persistently enigmatic nature of entanglement and EPR steering, they have been meticulously prepared, skillfully manipulated, and extensively utilized across a wide range of physical platforms, spanning from theoretical explorations [23–34] to experimental implementations [35–41]. The distinctive characteristic of EPR steering renders it highly significant for a multitude of quantum information protocols which depend on entanglement, offering additional security [42], such as semisided device-independent quantum key distribution [43–45], quantum secret sharing [35,46], one-way quantum computing [47], and subchannel discrimination [48]. EPR steering has been successfully achieved in various systems, including optomechanical systems [49–51], antiferromagnetic systems [35,52], cavity magnonic systems [53,54], and so on.

In recent years, all-optical systems have garnered widespread attention due to their unique advantages [55] and have been applied to various applications in quantum information processing, such as optical nonreciprocity [56], nonreciprocal photon blockade [57], and entanglement swapping [58]. This opens up broader prospects for applications in integrated photonics, photonic chips, and micro- and nano-optics. Among all-optical configurations, whispering-gallery-mode microring resonators possess several advantages, including a high-quality factor, low mode volume, and high optical density [59–61]. These characteristics make them highly attractive for studying light-matter interactions. They have emerged as versatile platforms for quantum physics research [56,57,62], offering a multitude of opportunities and remarkable achievements. These high-quality optical microring resonators, characterized by their weakly confined circulating modes, provide unique functionalities in a wide range of scientific and technological applications.

Motivated by the implications of these studies, in this paper we investigate the nonreciprocal quantum entanglement and

*Contact author: hfwang@ybu.edu.cn

†Contact author: yixx@nenu.edu.cn

one-way EPR steering in an all-optical system consisting of two coupled whispering-gallery-mode microring resonators R_A and R_B and two nearby optical waveguides. When the pumping field is input to R_A in the forward case, we find that the counterclockwise mode $b_{\circlearrowleft}$ generated in R_B satisfies the phase-matching condition with the two counterclockwise photons generated by the two-photon driving, resulting in the squeezing of the counterclockwise mode $b_{\circlearrowleft}$ in R_B, and thus the quantum correlations can be achieved. However, since the clockwise mode $b_{\circlearrowright}$ generated in R_B pumped in the backward case does not satisfy the phase-matching condition, the quantum correlations cannot be achieved. Therefore, we can only achieve quantum entanglement between a unique pair of optical modes, induced solely by the pumping field input from the forward case and two-photon driving, thus achieving perfect nonreciprocal quantum entanglement in the system. Moreover, the opposite frequency detunings, lower decay rates, and higher coupling strength between two optical modes significantly enhance both quantum entanglement and one-way EPR steering. Furthermore, the directionality of one-way EPR steering depends on the decay rates between two optical modes, where the mode with a lower decay rate is more likely to steer the other; in other words, the mode with a larger particle population is more easily steered by the other. Our work provides a promising platform for generating and controlling quantum entanglement and one-way EPR steering.

The paper is organized as follows. In Sec. II we introduce the physical model of the all-optical nonreciprocal system and derive the dynamics and the covariance matrix of this system. In Sec. III the generation and manipulation of nonreciprocal entanglement and one-way EPR steering between two optical modes are explicitly investigated. A summary is given in Sec. IV.

II. MODEL AND EQUATION OF MOTION

The schematic of the proposed system is depicted in Fig. 1, which consists of two coupled whispering-gallery-mode microring resonators and two adjacent optical waveguides. The resonator R_A undergoes continuous pumping field with frequency ω_L simultaneously from port 1 and port 2. The pumping field input from port 1 (forward-input case) excites the clockwise mode $a_{\circlearrowright}$ in R_A and the counterclockwise mode $b_{\circlearrowleft}$ in R_B. In the meantime, another pumping field input from port 2 (backward-input case) excites the counterclockwise mode $a_{\circlearrowleft}$ in R_A and the clockwise mode $b_{\circlearrowright}$ in R_B. Additionally, resonator R_B is subjected to a continuous two-photon driving field from port 3 with frequency $2\omega_L$ and amplitude Ω_b. This two-photon driving induces counterclockwise two-photon propagation in R_B. Due to phase-matching conditions in the parametric nonlinear process, the two-photon driving field squeezes the counterclockwise mode $b_{\circlearrowleft}$ excited by port 1, while the clockwise mode $b_{\circlearrowright}$ excited by port 2 remains unsqueezed, which is equivalent to the absence of nonlinear pumping in the entire system. The R_A slightly differs in size from R_B such that the two-photon driving cannot drive the parametric nonlinear process in the R_A; thus we only need to focus on the mode squeezing in R_B.

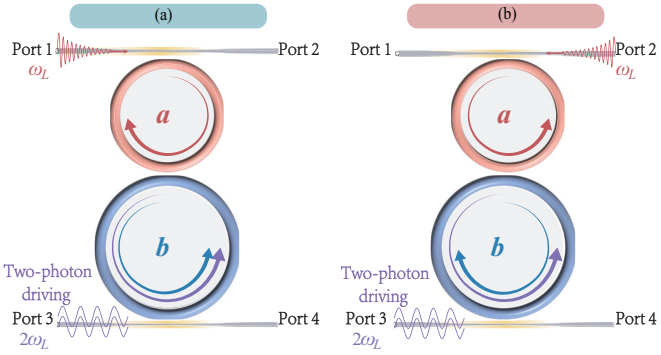

FIG. 1. Schematic of an all-optical nonreciprocal system comprising two microring resonators R_A and R_B and two adjacent optical waveguides. (a) A forward-input pumping field creates a clockwise mode $a_{\circlearrowright}$ in R_A and a counterclockwise mode $b_{\circlearrowleft}$ in R_B, which satisfy the phase-matching condition with the two counterclockwise photons generated by the two-photon driving. (b) A backward-input pumping field creates a counterclockwise mode $a_{\circlearrowleft}$ in R_A and a clockwise mode $b_{\circlearrowright}$ in R_B, which do not satisfy the phase-matching condition with the two counterclockwise photons generated by the two-photon driving.

For the forward-input case, the Hamiltonian of the system is written as ($\hbar = 1$)

$$H_{\rm fw} = H_{\rm sys} + H_{\rm dri}, \tag{1}$$

with

$$\begin{aligned} H_{\rm sys} &= \omega_a a^\dagger_{\circlearrowright} a_{\circlearrowright} + \omega_b b^\dagger_{\circlearrowleft} b_{\circlearrowleft} + J(a^\dagger_{\circlearrowright} b_{\circlearrowleft} + a_{\circlearrowright} b^\dagger_{\circlearrowleft}), \\ H_{\rm dri} &= \Omega_a (a^\dagger_{\circlearrowright} e^{-i\omega_L t} + \text{H.c.}) + \Omega_b (b^{\dagger 2}_{\circlearrowleft} e^{-2i\omega_L t} + \text{H.c.}). \end{aligned} \tag{2}$$

Here $a^\dagger_{\circlearrowright}$ and $b^\dagger_{\circlearrowleft}$ ($a_{\circlearrowright}$ and $b_{\circlearrowleft}$) are the creation (annihilation) operators of the R_A with frequency ω_a and the R_B with frequency ω_b, respectively, satisfying the standard commutation relations for bosons. The parameter J denotes the coherent coupling rate between two optical modes. Here $\Omega_a = \sqrt{2\kappa_a P_a/\omega_L}$ is the driving strength of the conventional signal with the input laser power P_a. Similarly, $\Omega_b = \sqrt{\kappa_b P_b/\omega_L}$ is the driving strength of the two-photon driving, where P_b is the input laser power and $\kappa_{a\,(b)}$ is the fiber-resonator coupling rate, i.e., decay rate of optical mode. In contrast, for the pumping field in the backward-input case for R_A, the Hamiltonian reads $H_{\rm bw} = \omega_a a^\dagger_{\circlearrowleft} a_{\circlearrowleft} + \omega_b b^\dagger_{\circlearrowleft} b_{\circlearrowleft} + J(a^\dagger_{\circlearrowleft} b_{\circlearrowleft} + a_{\circlearrowleft} b^\dagger_{\circlearrowleft}) + \Omega_a (a^\dagger_{\circlearrowleft} e^{-i\omega_l t} + \text{H.c.})$. Similarly, $a^\dagger_{\circlearrowleft}$ and $b^\dagger_{\circlearrowright}$ ($a_{\circlearrowleft}$ and $b_{\circlearrowright}$) are the creation (annihilation) operators of R_A for pumping in the the case of backward input. Comparing the Hamiltonians $H_{\rm fw}$ and $H_{\rm bw}$, we can observe that the primary distinction lies in the presence of the two-photon driving term. In other words, when the pumping field is input from the back, because the phase-matching condition is not satisfied, the two-photon driving has no effect in the whole system, i.e., $\Omega_b = 0$.

For convenience, we switch to the rotating frame with respect to the driving frequency ω_L, and by introducing input noises and dissipations of the system, the quantum Langevin equations (forward-input case) for the operators in the system

are given by

$$\begin{aligned}\dot{a}_{\circlearrowleft} &= -(i\Delta_a + \kappa_a)a_{\circlearrowleft} - iJb_{\circlearrowleft} - i\Omega_a + \sqrt{2\kappa_a}a^{\text{in}},\\ \dot{b}_{\circlearrowleft} &= -(i\Delta_b + \kappa_b)b_{\circlearrowleft} - iJa_{\circlearrowleft} - 2i\Omega_b b^{\dagger}_{\circlearrowleft} + \sqrt{2\kappa_b}b^{\text{in}}\end{aligned} \quad (3)$$

and the quantum Langevin equations (backward-input case) for two operators are given by

$$\begin{aligned}\dot{a}_{\circlearrowleft} &= -(i\Delta_a + \kappa_a)a_{\circlearrowleft} - iJb_{\circlearrowleft} - i\Omega_a + \sqrt{2\kappa_a}a^{\text{in}},\\ \dot{b}_{\circlearrowleft} &= -(i\Delta_b + \kappa_b)b_{\circlearrowleft} - iJa_{\circlearrowleft} + \sqrt{2\kappa_b}b^{\text{in}},\end{aligned} \quad (4)$$

where $\Delta_{a\,(b)} = \omega_{a\,(b)} - \omega_L$ is the frequency detuning of $R_{A\,(B)}$. The input noise operators a^{in} and b^{in} are zero mean and are characterized by the correlation functions

$$\begin{aligned}\langle a^{\text{in}\dagger}(t)a^{\text{in}}(t')\rangle &= n_a\delta(t-t'),\\ \langle a^{\text{in}}(t)a^{\text{in}\dagger}(t')\rangle &= (n_a+1)\delta(t-t'),\\ \langle b^{\text{in}\dagger}(t)b^{\text{in}}(t')\rangle &= n_b\delta(t-t'),\\ \langle b^{\text{in}}(t)b^{\text{in}\dagger}(t')\rangle &= (n_b+1)\delta(t-t'),\end{aligned} \quad (5)$$

where $n_{a\,(b)} = (e^{\hbar\omega_{a\,(b)}/k_BT} - 1)^{-1}$ are the mean thermal excitation numbers in the environmental temperature T, with k_B the Boltzmann constant.

To quantify quantum entanglement and EPR steering between two optical modes, we introduce two sets of quadrature components $X_a^{(\text{in})}$ and $Y_a^{(\text{in})}$, and $X_b^{(\text{in})}$ and $Y_b^{(\text{in})}$, which are defined as

$$\begin{aligned}X_a^{(\text{in})} &= \frac{a^{(\text{in})} + a^{(\text{in})\dagger}}{\sqrt{2}}, \quad Y_a^{(\text{in})} = \frac{a^{(\text{in})} - a^{(\text{in})\dagger}}{i\sqrt{2}},\\ X_b^{(\text{in})} &= \frac{b^{(\text{in})} + b^{(\text{in})\dagger}}{\sqrt{2}}, \quad Y_b^{(\text{in})} = \frac{b^{(\text{in})} - b^{(\text{in})\dagger}}{i\sqrt{2}}.\end{aligned} \quad (6)$$

The above calculations of quadrature components are applicable to any of the four types of photon circulation modes (i.e., $a_{\circlearrowleft}$, $a_{\circlearrowleft}$, $b_{\circlearrowleft}$, and $b_{\circlearrowleft}$) we mentioned. Then the quantum Langevin equations can be written in the compact matrix form

$$\dot{\sigma}(t) = \mathcal{A}\sigma(t) + \varrho(t), \quad (7)$$

with $\sigma = [X_a, Y_a, X_b, Y_b]^T$ and $\varrho = [\sqrt{2\kappa_a}X_a^{\text{in}}, \sqrt{2\kappa_a}Y_a^{\text{in}}, \sqrt{2\kappa_b}X_b^{\text{in}}, \sqrt{2\kappa_b}Y_b^{\text{in}}]^T$ the vectors of quantum operators and noises, respectively. The drift matrix $\mathcal{A}$ reads

$$\mathcal{A} = \begin{pmatrix} -\kappa_a & \Delta_a & 0 & J \\ -\Delta_a & -\kappa_a & -J & 0 \\ 0 & J & -\kappa_b & \Delta_b - 2\Omega_b \\ -J & 0 & -\Delta_b - 2\Omega_b & -\kappa_b \end{pmatrix}. \quad (8)$$

Due to the linearity of the Langevin equations and the Gaussian nature of the quantum noises, the system will decay to a stationary Gaussian state, which can be completely characterized by a 4×4 covariance matrix (CM) $\mathcal{V}$ in the phase space $\mathcal{V}_{ij} = \langle\sigma_i(t)\sigma_j(t') + \sigma_j(t')\sigma_i(t)\rangle/2$ ($i, j = 1, 2, 3, 4$). The steady-state CM $\mathcal{V}$ can be obtained straightforwardly by solving the Lyapunov equation, with $\mathcal{D}_{ij}\delta(t-t') = \langle\sigma_i(t)\sigma_j(t') + \sigma_j(t')\sigma_i(t)\rangle/2$.

For the continuous-variable two-mode Gaussian state, a computable criterion of EPR steering based on quantum coherent information has been introduced [22]. For quantum entanglement, it is convenient to use the logarithmic negativity E_N to quantify its level [63]. Note that all the above-mentioned measures can be computed from the 4×4 CM for two optical modes

$$\mathcal{V} = \begin{pmatrix} \mathcal{V}_1 & \mathcal{V}_3 \\ \mathcal{V}_3^T & \mathcal{V}_2 \end{pmatrix}, \quad (9)$$

where $\mathcal{V}_1$, $\mathcal{V}_2$, and $\mathcal{V}_3$ are 2×2 subblock matrices of $\mathcal{V}$. The definition of logarithmic negativity E_N is expressed as

$$E_N \equiv \max[0, -\ln(2\nu)], \quad (10)$$

where $\nu = \sqrt{\mathcal{E} - (\mathcal{E}^2 - 4\mathcal{R})^{1/2}}/\sqrt{2}$ and $\mathcal{E} = \mathcal{R}_1 + \mathcal{R}_2 - 2\mathcal{R}_3$. with $\mathcal{R}_1 = \det\mathcal{V}_1$, $\mathcal{R}_2 = \det\mathcal{V}_2$, $\mathcal{R}_3 = \det\mathcal{V}_3$, and $\mathcal{R} = \det\mathcal{V}$ symplectic invariants. Moreover, the quantification of EPR steering has been introduced for arbitrary two-mode Gaussian states of a continuous-variable system [25]. The quantum steerabilities of Gaussian modes $a \to b$ and $b \to a$ are quantified as [26]

$$\begin{aligned}\mathcal{G}_{a\to b} &\equiv \max\left[0, \frac{1}{2}\ln\frac{\mathcal{R}_1}{4\mathcal{R}}\right],\\ \mathcal{G}_{b\to a} &\equiv \max\left[0, \frac{1}{2}\ln\frac{\mathcal{R}_2}{4\mathcal{R}}\right]\end{aligned} \quad (11)$$

respectively. If $\mathcal{G}_{a\to b} > \mathcal{G}_{b\to a}$ ($\mathcal{G}_{b\to a} < \mathcal{G}_{a\to b}$), it suggests that optical mode a (b) can steer optical mode b (a) through Gaussian measurements, and this value measures the extent of EPR steering. In other words, a higher-$\mathcal{G}$ value indicates stronger Gaussian steerability. To better explain the directionality of the one-way EPR steering between two optical modes, we introduce the mode populations, i.e., the final mean photon numbers, which can be obtained from the relation $P_o = \frac{1}{2}(\langle\delta X^2_{a\,(b)}\rangle + \langle\delta Y^2_{a\,(b)}\rangle - 1)$.

III. RESULTS AND DISCUSSION

In this section we numerically simulate the behavior of the quantum entanglement and EPR steering in the parameter space by employing E_N and $\mathcal{G}_{a\to b}$ ($\mathcal{G}_{b\to a}$). All the results are obtained in the steady state, which is guaranteed by the negative eigenvalues (real parts) of the drift matrix $\mathcal{A}$. We investigate the dependence of E_N on the parameter Δ_a for the forward-input case and backward-input case as shown in Fig. 2. Here we choose identical resonant frequencies $\omega_a/2\pi = \omega_b/2\pi = 193.4$ THz and damping rates $\kappa_a/2\pi = \kappa_b/2\pi = 5$ MHz and we set the environmental temperature $T = 20$ mK in all the following discussion. From Fig. 2 we can observe intuitively that when the coupling strength between two optical modes is $J/2\pi = 15$ MHz, for the case where the pumping field is input from the front ($\Omega_b/2\pi = 11.5$ MHz), the quantum entanglement E_{N1} between modes $a_{\circlearrowleft}$ and $b_{\circlearrowleft}$ can be effectively prepared. The E_{N1} (blue solid line) increases with the frequency detuning $\Delta_a/2\pi$ and reaches its maximum value $E_{N1} \approx 0.22$ when the frequency detuning $\Delta_a/2\pi$ is roughly 115 MHz. Afterward, the E_{N1} gradually decreases with the increase of frequency detuning Δ_a. In contrast, for the case where the pumping field is input from the back ($\Omega_b = 0$), the E_{N2} between modes $a_{\circlearrowleft}$ and $b_{\circlearrowleft}$ keeps a constant zero value, which means that there is no

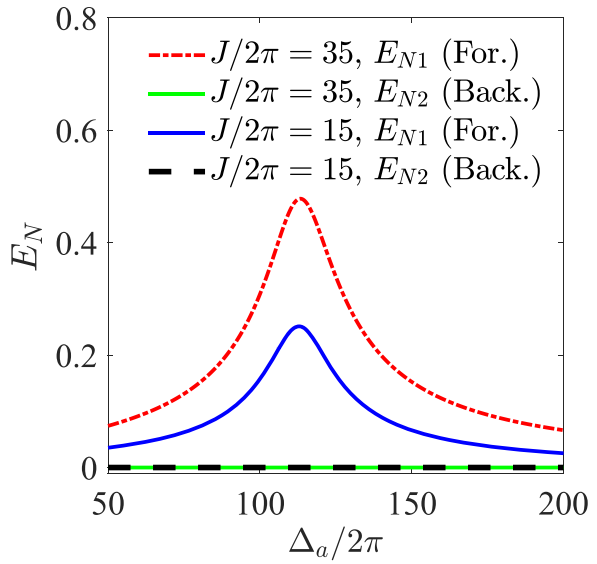

FIG. 2. Quantum entanglement E_N as a function of frequency detuning Δ_a for the cases of pumping field only input from the front ($\Omega_b/2\pi = 11.5$ MHz) and only input from the back ($\Omega_b = 0$) with different coupling strengths J. The other parameters are $\kappa_a/2\pi = \kappa_b/2\pi = 5$ MHz, $\Delta_b/2\pi = -115$ MHz, and $T = 20$ mK.

quantum entanglement E_{N2} even if the frequency detuning increases (black dashed line).

Similarly, when we introduce a stronger coherent coupling rate $J/2\pi = 35$ MHz, the evolution of quantum entanglement is exactly the same for the case of a coherent coupling rate $J/2\pi = 15$ MHz for two input cases. The quantum entanglement E_{N1} exhibits a similar trend, increasing and then decreasing with the increase of frequency detuning Δ_a; the difference is that the maximum entanglement at $\Delta_a/2\pi = 115$ MHz reaches 0.5 (red dash-dotted line). However, for the case of input from the back ($\Omega_b = 0$), we still cannot achieve quantum entanglement E_{N2} between two optical modes (green solid line). Therefore, we conclude that the existence of the two-photon driving term is necessary to generate quantum entanglement. In other words, in our designed system model, pumping driving from two ports simultaneously excite two pairs of tunneling-coupled photon circulation modes, but only the $b_{\circlearrowleft}$ mode excited from port 1 satisfies the phase-matching condition with the photon circulation excited by the two-photon driving. Therefore, even with continuous pumping input from port 2, we can only ever produce quantum entanglement E_{N1} between $a_{\circlearrowleft}$ and $b_{\circlearrowleft}$ excited by port 1, thus achieving nonreciprocal quantum entanglement. Additionally, for the case of input from port 1, a higher coupling rate J significantly enhances the quantum entanglement. However, for the case of input from the back, we are unable to obtain quantum entanglement because there is no two-photon driving term $\Omega_b(b_{\circlearrowleft}^{\dagger 2} + b_{\circlearrowleft}^2)$ in the system, i.e., $\Omega_b = 0$. The validity of this nonlinear term can only be ensured by the pumping field input from the front near R_A.

According to the analysis of the quantum entanglement in Fig. 2, we draw the conclusion that the only nonreciprocal quantum entanglement obtained in this scheme can be prepared only when the pumping field is input from port 1 and the two-photon driving is input from port 3. Therefore, we only focus on the case where the pumping field is input from the forward end to R_A. We plot Fig. 3 to further illustrate the evolution of quantum entanglement between two optical modes with respect to several parameters such as frequency detunings, coupling strength, driving strength, and decay rates for the forward-input case. In Fig. 3(a) it is quite evident that the quantum entanglement can be achieved under a very broad range of frequency detuning parameter conditions. The quantum entanglement is particularly obvious when the frequency detunings of the two optical modes are opposite ($\Delta_a = -\Delta_b$). The maximum entanglement occurs at $\Delta_a/2\pi = -\Delta_b/2\pi \approx 115$ MHz, which corresponds precisely to the results shown in Fig. 2. Considering these optimal frequency detunings, we further investigate the impact of coupling strength J and two-photon driving strength Ω_b on entanglement, as shown in Fig. 3(b). The results clearly demonstrate that both the higher coupling strength and the two-photon driving strength contribute to enhance quantum entanglement. Conversely, as depicted in Fig. 3(c), when the decay rates of two optical modes are lower, the higher degree of quantum entanglement can be achieved.

In order to study the nonreciprocal quantum entanglement in more detail, it is essential to elucidate the mechanism behind the implementation using two-photon driving. For this purpose, we proceed via the rotated Hamiltonian in the case of forward input

$$\begin{aligned} H_{\rm rot} =& \Delta_a a_{\circlearrowleft}^{\dagger} a_{\circlearrowleft} + \Delta_b b_{\circlearrowleft}^{\dagger} b_{\circlearrowleft} + J(a_{\circlearrowleft}^{\dagger} b_{\circlearrowleft} + a_{\circlearrowleft} b_{\circlearrowleft}^{\dagger}) \\ &+ \Omega_a(a_{\circlearrowleft}^{\dagger} + a_{\circlearrowleft}) + \Omega_b(b_{\circlearrowleft}^{\dagger 2} + b_{\circlearrowleft}^2), \end{aligned} \tag{12}$$

whereafter we diagonalize the Hamiltonian by introducing Bogoliubov modes

$$\begin{aligned} \beta &= S^{\dagger}(r) b_{\circlearrowleft} S(r) = b_{\circlearrowleft} \cosh r + b_{\circlearrowleft}^{\dagger} \sinh r, \\ \beta^{\dagger} &= S^{\dagger}(r) b_{\circlearrowleft}^{\dagger} S(r) = b_{\circlearrowleft}^{\dagger} \cosh r + b_{\circlearrowleft} \sinh r, \end{aligned} \tag{13}$$

where $|\tanh 2r| = |2\Omega_b/\Delta_b|$ and $r = \frac{1}{4}\ln[(1+\beta)/(1-\beta)]$ is the coefficient of compressibility. This also satisfies the bosonic commutation relation $[\beta, \beta^{\dagger}] = 1$. The effective Hamiltonian of the system can be rewritten as

$$\begin{aligned} \mathcal{H}_{\rm eff} =& \Delta_a a_{\circlearrowleft}^{\dagger} a_{\circlearrowleft} + \Delta_{\beta} \beta^{\dagger} \beta + J_+(\beta^{\dagger} a_{\circlearrowleft} + \beta a^{\dagger}) \\ &+ J_-(\beta^{\dagger} a_{\circlearrowleft}^{\dagger} + \beta a_{\circlearrowleft}) + \Omega_a(a_{\circlearrowleft}^{\dagger} + a_{\circlearrowleft}), \end{aligned} \tag{14}$$

where $\Delta_{\beta} = \sqrt{\Delta_b^2 - 4\Omega_b^2}$, $J_+ = J\cosh r$, and $J_- = J\sinh r$. In other words, in the presence of the two-photon driving term, we can achieve adjustable frequency detuning and coupling strength. The forward input of the pumping field satisfies the phase-matching condition, thus ensuring the validity of the nonlinear driving. According to the Hamiltonian given by the Eq. (14), the parametric-type interaction term $\beta^{\dagger} a_{\circlearrowleft}^{\dagger} + \beta a_{\circlearrowleft}$ is essential for implementing quantum entanglement. It is worth noting that the particularly obvious quantum entanglement between two optical modes can be achieved when the optimal detuning of the two optical modes satisfies $\Delta_a = -\Delta_{\beta}$, which is in excellent agreement with Fig. 3(a). Meanwhile, the state-swap interaction between two optical modes is also enhanced because of $J\cosh r > J$ for $r > 0$. Thus, the quantum entanglement between two optical modes arises from

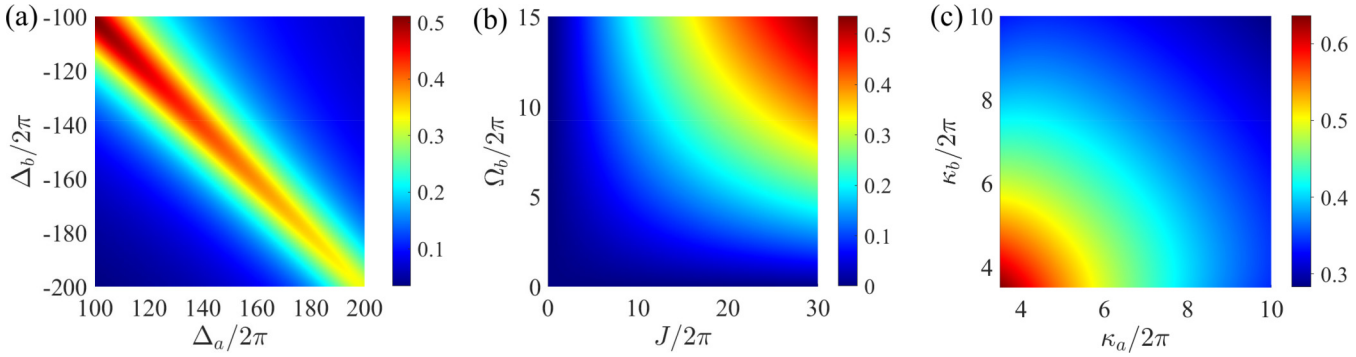

FIG. 3. Density plot of quantum entanglement E_N as a function of (a) frequency detunings Δ_a and Δ_b, (b) coupling strength J and driving strength Ω_b, and (c) decay rates κ_a and κ_b, with (a) and (c) $J/2\pi = 35$ MHz and $\Omega_b/2\pi = 11.5$ MHz and (b) and (c) $\Delta_a/2\pi = 115$ MHz. The other parameters are the same as those in Fig. 2.

the parametric-type interaction induced by the two-photon driving term $\Omega_b(b_{\circlearrowleft}^{\dagger 2} + b_{\circlearrowleft}^{2})$. In contrast, for the pumping field in the backward-input case for R_A, the two-photon driving has no effect on the clockwise mode b. Therefore, in this case, due to the absence of a nonlinear driving term, there is no quantum entanglement E_{N2} between two optical modes, as shown by the green dashed line and black solid line in Fig. 2.

Now we turn to analyze the generation and manipulation of one-way EPR steering. We note that the EPR steerings $\mathcal{G}_{a\to b}$ and $\mathcal{G}_{b\to a}$, as a strict subset of quantum entanglement, can also be obtained in the system and are depicted as a function of κ_a and κ_b in Figs. 4(a) and 4(b), respectively. We can find that the EPR steering $\mathcal{G}_{a\to b}$ can be obtained when the relation of the decay rates is $\kappa_b > \kappa_a$; however, as for $\mathcal{G}_{b\to a}$, it can be obtained in the region of $\kappa_a > \kappa_b$. More specifically, the EPR steerings $\mathcal{G}_{a\to b}$ and $\mathcal{G}_{b\to a}$ appear in the regions where the decay rates are asymmetrical; further,

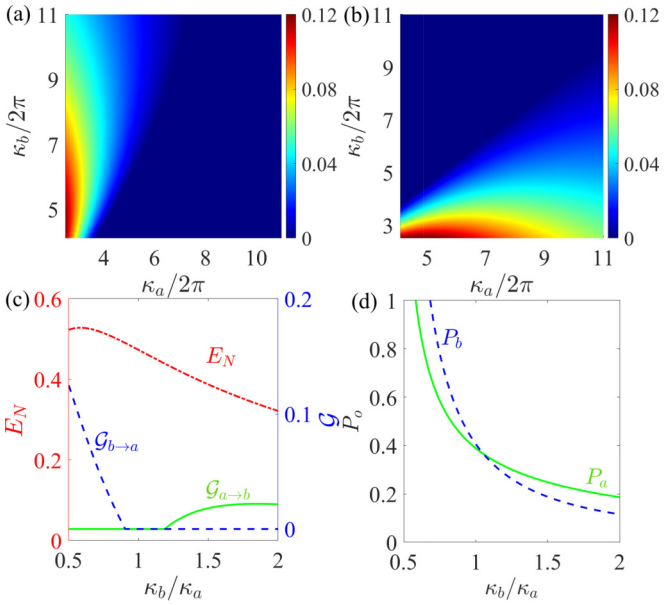

FIG. 4. Quantum steering (a) $\mathcal{G}_{a\to b}$ and (b) $\mathcal{G}_{b\to a}$ as a function of κ_a and κ_b. (c) Quantum entanglement E_N, steering $\mathcal{G}_{a\to b}$, and steering $\mathcal{G}_{b\to a}$ and (d) populations of two modes P_a and P_b versus κ_b/κ_a with $\kappa_a/2\pi = 5$ MHz. The other parameters are the same as those in Fig. 3(c).

the mode with lower decay rate is more difficult to steer by the other mode. Consequently, the desired one-way EPR steering can be achieved by adjusting the decay rates of the two optical modes. Figure 4(c) shows the effects of κ_b on quantum entanglement and one-way EPR steering for a fixed κ_a. One can observe that the quantum entanglement decreases as κ_b increases, which corresponds exactly to the result in Fig. 3(c), namely, on the premise of ensuring the stability of the system, when the decay rate of the system is lower, there is less energy loss, resulting in a greater degree of quantum entanglement. As for one-way EPR steering, when the decay rates of two optical modes are roughly equal, i.e., $\kappa_b/\kappa_a \approx 1$, there is no one-way steering $\mathcal{G}_{a\to b}$ and $\mathcal{G}_{b\to a}$ in the system. In contrast, when the decay rates between two optical modes satisfy $\kappa_b/\kappa_a < 1$, the achievement of one-way EPR steering $\mathcal{G}_{b\to a}$ is enabled; conversely, when the decay rates between two optical modes satisfy $\kappa_b/\kappa_a > 1$, one-way EPR steering $\mathcal{G}_{a\to b}$ is allowed. These observations align with the results presented in Figs. 4(a) and 4(b). It is evident that when the decay rates are nearly identical ($\kappa_a \approx \kappa_b$), the two optical modes have nearly equal particle populations, resulting in the absence of one-way EPR steering between two optical modes, as illustrated in Figs. 4(c) and 4(d). The result comes from the fact that the mode with larger population is more difficult to steer by the other mode.

We further investigate the one-way EPR steering $\mathcal{G}_{a\to b}$ as a function of frequency detunings Δ_a and Δ_b, coupling strength J, and driving strength Ω_b in Figs. 5(a) and 5(b). Under the current parameter conditions, one-way EPR steering $\mathcal{G}_{b\to a}$ does not exist, so we do not presented it here. We can see that the one-way EPR steering as a strict subset of quantum entanglement has similar properties to quantum entanglement. The one-way EPR steering $\mathcal{G}_{a\to b}$, which is the same as the quantum entanglement, can be obtained in large quantities when $\Delta_a = -\Delta_b$ and reaches its maximum value when $\Delta_a/2\pi = -\Delta_b/2\pi \approx 115$ MHz. On the other hand, it can also achieve larger values with the greater coupling strength J and the two-photon driving strength Ω_b. In the following, we plot the quantum entanglement E_N and one-way EPR steerings $\mathcal{G}_{a\to b}$ and $\mathcal{G}_{b\to a}$ as functions of Δ_b/Δ_a in Fig. 5(c). It can be observed that quantum entanglement initially increases as Δ_b/Δ_a rises, reaching its peak at $\Delta_a = -\Delta_b$ and subsequently decreasing for larger values of Δ_b/Δ_a. This implies that once beyond the optimal value of $\Delta_a = -\Delta_b$,

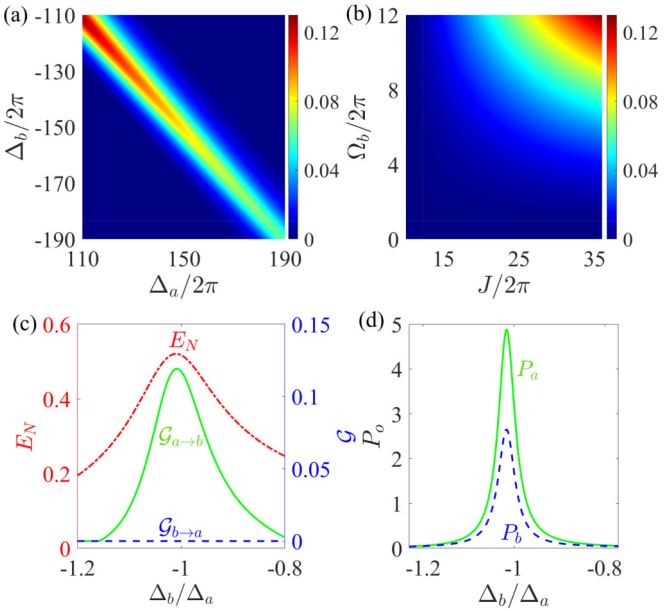

FIG. 5. Quantum steering $\mathcal{G}_{a\to b}$ as a function of (a) detunings Δ_a and Δ_b and (b) coupling strength J and driving strength Ω_b. (c) Quantum entanglement E_N and one-way steering ($\mathcal{G}_{a\to b}$ and $\mathcal{G}_{b\to a}$) and (d) populations of two optical modes P_a and P_b as a function of Δ_b/Δ_a. In all panels $\kappa_b/2\pi = 2\kappa_a/2\pi = 5$ MHz; the other parameters are the same as those in Fig. 3(c).

the continuous enhancement of Δ_b/Δ_a has a destructive effect on the quantum entanglement. For the one-way EPR steering $\mathcal{G}_{a\to b}$, it has a very similar evolution behavior to quantum entanglement; specifically, $\mathcal{G}_{a\to b}$ is more perfectly prepared only if the frequency detunings are very close to $\Delta_a = -\Delta_b$ [see Fig. 5(a)], but the limits of entanglement are relatively broad. In addition, since the current parameter is set $\kappa_a < \kappa_b$, the one-way EPR steering $\mathcal{G}_{b\to a}$ does not exist in the system, which corresponds exactly to the results of Fig. 4(c). In the same way, the populations of two optical modes P_a and P_b as a function of the ratio Δ_b/Δ_a are shown in Fig. 5(d), which also confirms that the mode with larger population is more difficult to steer by the other mode.

IV. CONCLUSION

We have proposed an advanced all-optical scheme consisting of a system of multile ports and dual-microring resonators to investigate the intriguing nonreciprocity of quantum entanglement and accomplish the precise preparation of one-way EPR steering. In this scheme, the counterclockwise mode $b_{\circlearrowleft}$ excited at port 1 aligns perfectly with the propagation direction of photons injected by the two-photon driving from port 3, thus facilitating a nonlinear parametric amplification process within the system. Remarkably, under the optimal conditions, the quantum entanglement is effectively prepared when the opposite frequency detunings are exhibited by two optical modes. Within this operational regime, a remarkably wide parameter space reveals the existence of a distinct region characterized by one-way EPR steering, firmly establishing the ability to exert full control over the quantum entanglement and EPR steering between two optical modes. Notably, the directionality of EPR steering can be fine-tuned by manipulating the dissipation rates of two optical modes, as evidenced by the striking correspondence between higher mode populations and enhanced degree of EPR steering.

However, when the pumping field is injected only from port 2 into R_A, the propagation directions of photons are completely opposite to that of the counterclockwise mode $b_{\circlearrowleft}$ excited by port 3. Therefore, according to the directional phase-matching condition, the system exhibits an equivalent behavior to a dual-mode optical system without nonlinear pumping. At this point, we can never achieve quantum entanglement E_{N2} coming from port 2 and port 3. However, due to the continuous input of the pump field at port 1, the system only produces quantum entanglement E_{N1} coming from port 1 and port 3, thereby achieving nonreciprocal quantum entanglement in the system. Importantly, since the resonant frequencies of two whispering-gallery-mode microring resonators are in the optical frequency range, both quantum entanglement and one-way EPR steering in our scheme can be fully prepared at room temperature ($T \approx 300$ K) and remain robust even when affected by increasing external environmental temperatures, which is highly advantageous for experimental implementations. With its inherent potential, our proposal not only offers a promising avenue for the coherent manipulation of quantum entanglement and the precise preparation of one-way EPR steering, but also holds profound implications for the development of macroscopic chiral quantum information.

ACKNOWLEDGMENTS

This work was supported by the Natural Science Foundation of Jilin Province through Grant No. 20240101013JC and the National Natural Science Foundation of China through Grants No. 12074330, No. 12375020, and No. 12175033.

[1] R. Raussendorf and H. J. Briegel, A one-way quantum computer, Phys. Rev. Lett. **86**, 5188 (2001).
[2] E. Knill, R. Laflamme, and G. J. Milburn, A scheme for efficient quantum computation with linear optics, Nature (London) **409**, 46 (2001).
[3] T. D. Ladd, F. Jelezko, R. Laflamme, Y. Nakamura, C. Monroe, and J. L. O'Brien, Quantum computers, Nature (London) **464**, 45 (2010).
[4] T. Albash and D. A. Lidar, Adiabatic quantum computation, Rev. Mod. Phys. **90**, 015002 (2018).
[5] V. Giovannetti, S. Lloyd, and L. Maccone, Quantum metrology, Phys. Rev. Lett. **96**, 010401 (2006).
[6] V. Giovannetti, S. Lloyd, and L. Maccone, Advances in quantum metrology, Nat. Photon. **5**, 222 (2011).
[7] S. Pirandola, J. Eisert, C. Weedbrook, A. Furusawa, and S. L. Braunstein, Advances in quantum teleportation, Nat. Photon. **9**, 641 (2015).

[8] R. Horodecki, P. Horodecki, M. Horodecki, and K. Horodecki, Quantum entanglement, Rev. Mod. Phys. **81**, 865 (2009).

[9] U. L. Andersen, G. Leuchs, and C. Silberhorn, Continuous-variable quantum information processing, Laser Photon. Rev. **4**, 337 (2010).

[10] F. Flamini, N. Spagnolo, and F. Sciarrino, Photonic quantum information processing: A review, Rep. Prog. Phys. **82**, 016001 (2019).

[11] C. L. Degen, F. Reinhard, and P. Cappellaro, Quantum sensing, Rev. Mod. Phys. **89**, 035002 (2017).

[12] J. Li, S. Y. Zhu, and G. S. Agarwal, Magnon-photon-phonon entanglement in cavity magnomechanics, Phys. Rev. Lett. **121**, 203601 (2018).

[13] M. Yu, H. Shen, and J. Li, Magnetostrictively induced stationary entanglement between two microwave fields, Phys. Rev. Lett. **124**, 213604 (2020).

[14] C. H. Bai, D. Y. Wang, S. Zhang, S. T. Liu, and H. F. Wang, Modulation-based atom-mirror entanglement and mechanical squeezing in an unresolved-sideband optomechanical system, Ann. Phys. (Berlin) **531**, 1800271 (2019).

[15] T. Wang, L. Wang, Y. M. Liu, C. H. Bai, D. Y. Wang, H. F. Wang, and S. Zhang, Temperature-resistant generation of robust entanglement with blue-detuning driving and mechanical gain, Opt. Express **27**, 29581 (2019).

[16] C. H. Bai, D. Y. Wang, S. Zhang, S. T. Liu, and H. F. Wang, Generation of strong mechanical-mechanical entanglement by pump modulation, Adv. Quantum Technol. **4**, 2000149 (2021).

[17] J. P. Dowling and G. J. Milburn, Quantum technology: The second quantum revolution, Philos. Trans. R. Soc. A **361**, 1655 (2003).

[18] E. Schrödinger, Discussion of probability relations between separated systems, Proc. Cambridge Philos. Soc. **31**, 555 (1935).

[19] H. M. Wiseman, S. J. Jones, and A. C. Doherty, Steering, entanglement, nonlocality, and the Einstein-Podolsky-Rosen paradox, Phys. Rev. Lett. **98**, 140402 (2007).

[20] Q. Y. He, L. Rosales-Zárate, G. Adesso, and M. D. Reid, Secure continuous variable teleportation and Einstein-Podolsky-Rosen steering, Phys. Rev. Lett. **115**, 180502 (2015).

[21] N. Brunner, D. Cavalcanti, S. Pironio, V. Scarani, and S. Wehner, Bell nonlocality, Rev. Mod. Phys. **86**, 419 (2014).

[22] I. Kogias, A. R. Lee, S. Ragy, and G. Adesso, Quantification of Gaussian quantum steering, Phys. Rev. Lett. **114**, 060403 (2015).

[23] P. Skrzypczyk, M. Navascués, and D. Cavalcanti, Quantifying Einstein-Podolsky-Rosen steering, Phys. Rev. Lett. **112**, 180404 (2014).

[24] M. K. Olsen and A. S. Bradley, Bright bichromatic entanglement and quantum dynamics of sum frequency generation, Phys. Rev. A **77**, 023813 (2008).

[25] A. Mari and J. Eisert, Gently modulating optomechanical systems, Phys. Rev. Lett. **103**, 213603 (2009).

[26] Q. Y. He and M. D. Reid, Einstein-Podolsky-Rosen paradox and quantum steering in pulsed optomechanics, Phys. Rev. A **88**, 052121 (2013).

[27] M. Wang, Q. H. Gong, Z. Ficek, and Q. Y. He, Role of thermal noise in tripartite quantum steering, Phys. Rev. A **90**, 023801 (2014).

[28] S. L. W. Midgley, A. J. Ferris, and M. K. Olsen, Asymmetric Gaussian steering: When Alice and Bob disagree, Phys. Rev. A **81**, 022101 (2010).

[29] M. K. Olsen, Asymmetric Gaussian harmonic steering in second-harmonic generation, Phys. Rev. A **88**, 051802(R) (2013).

[30] J. Schneeloch, C. J. Broadbent, S. P. Walborn, E. G. Cavalcanti, and J. C. Howell, Einstein-Podolsky-Rosen steering inequalities from entropic uncertainty relations, Phys. Rev. A **87**, 062103 (2013).

[31] D. A. Evans and H. M. Wiseman, Optimal measurements for tests of Einstein-Podolsky-Rosen steering with no detection loophole using two-qubit Werner states, Phys. Rev. A **90**, 012114 (2014).

[32] L. Rosales-Zárate, R. Y. Teh, S. Kiesewetter, A. Brolis, K. Ng, and M. D. Reid, Decoherence of Einstein-Podolsky-Rosen steering, J. Opt. Soc. Am. B **32**, A82 (2015).

[33] J. Bowles, T. Vértesi, M. T. Quintino, and N. Brunner, One-way Einstein-Podolsky-Rosen steering, Phys. Rev. Lett. **112**, 200402 (2014).

[34] Q. Y. He, Q. H. Gong, and M. D. Reid, Classifying directional Gaussian entanglement, Einstein-Podolsky-Rosen steering, and discord, Phys. Rev. Lett. **114**, 060402 (2015).

[35] S. Armstrong, M. Wang, R. Y. Teh, Q. H. Gong, Q. Y. He, J. Janousek, H. A. Bachor, M. D. Reid, and P. K. Lam, Multipartite Einstein-Podolsky-Rosen steering and genuine tripartite entanglement with optical networks, Nat. Phys. **11**, 167 (2015).

[36] V. Händchen, T. Eberle, S. Steinlechner, A. Samblowski, T. Franz, R. F. Werner, and R. Schnabel, Observation of one-way Einstein-Podolsky-Rosen steering, Nat. Photon. **6**, 596 (2012).

[37] Z. Z. Qin, X. W. Deng, C. X. Tian, M. H. Wang, X. L. Su, C. D. Xie, and K. C. Peng, Manipulating the direction of Einstein-Podolsky-Rosen steering, Phys. Rev. A **95**, 052114 (2017).

[38] K. Sun, X. J. Ye, J. S. Xu, X. Y. Xu, J. S. Tang, Y. C. Wu, J. L. Chen, C. F. Li, and G. C. Guo, Experimental quantification of asymmetric Einstein-Podolsky-Rosen steering, Phys. Rev. Lett. **116**, 160404 (2016).

[39] S. Wollmann, N. Walk, A. J. Bennet, H. M. Wiseman, and G. J. Pryde, Observation of genuine one-way Einstein-Podolsky-Rosen steering, Phys. Rev. Lett. **116**, 160403 (2016).

[40] Y. Xiao, X. J. Ye, K. Sun, J. S. Xu, C. F. Li, and G. C. Guo, Demonstration of multisetting one-way Einstein-Podolsky-Rosen steering in two-qubit systems, Phys. Rev. Lett. **118**, 140404 (2017).

[41] N. Tischler, F. Ghafari, T. J. Baker, S. Slussarenko, R. B. Patel, M. M. Weston, S. Wollmann, L. K. Shalm, V. B. Verma, S. W. Nam, H. C. Nguyen, H. M. Wiseman, and G. J. Pryde, Conclusive experimental demonstration of one-way Einstein-Podolsky-Rosen steering, Phys. Rev. Lett. **121**, 100401 (2018).

[42] B. Opanchuk, L. Arnaud, and M. D. Reid, Detecting faked continuous-variable entanglement using one-sided device-independent entanglement witnesses, Phys. Rev. A **89**, 062101 (2014).

[43] C. Branciard, E. G. Cavalcanti, S. P. Walborn, V. Scarani, and H. M. Wiseman, One-sided device-independent quantum key distribution: Security, feasibility, and the connection with steering, Phys. Rev. A **85**, 010301(R) (2012).

[44] T. Gehring, V. Händchen, J. Duhme, F. Furrer, T. Franz, C. Pacher, R. F. Werner, and R. Schnabel, Implementation of continuous-variable quantum key distribution with composable and one-sided-device-independent security against coherent attacks, Nat. Commun. **6**, 8795 (2015).

[45] N. Walk, S. Hosseni, J. Geng, O. Thearle, J. Y. Haw, S. Armstrong, S. M. Assad, J. Janousek, T. C. Ralph, T. Symul, H. M. Wiseman, and P. K. Lam, Experimental demonstration of Gaussian protocols for one-sided device-independent quantum key distribution, Optica **3**, 634 (2016).

[46] I. Kogias, Y. Xiang, Q. Y. He, and G. Adesso, Unconditional security of entanglement-based continuous-variable quantum secret sharing, Phys. Rev. A **95**, 012315 (2017).

[47] C. M. Li, K. Chen, Y. N. Chen, Q. Zhang, Y. A. Chen, and J. W. Pan, Genuine high-order Einstein-Podolsky-Rosen steering, Phys. Rev. Lett. **115**, 010402 (2015).

[48] M. Piani and J. Watrous, Necessary and sufficient quantum information characterization of Einstein-Podolsky-Rosen steering, Phys. Rev. Lett. **114**, 060404 (2015).

[49] J. El Qars, M. Daoud, and R. Ahl Laamara, Controlling stationary one-way steering via thermal effects in optomechanics, Phys. Rev. A **98**, 042115 (2018).

[50] C. G. Liao, H. Xie, R. X. Chen, M. Y. Ye, and X. M. Lin, Controlling one-way quantum steering in a modulated optomechanical system, Phys. Rev. A **101**, 032120 (2020).

[51] Q. Guo, M. R. Wei, C. H. Bai, Y. Zhang, G. Li, and T. Zhang, Manipulation and enhancement of Einstein-Podolsky-Rosen steering between two mechanical modes generated by two Bogoliubov dissipation pathways, Phys. Rev. Res. **5**, 013073 (2023).

[52] S. S. Zheng, F. X. Sun, Y. J. Lai, Q. H. Gong, and Q. Y. He, Manipulation and enhancement of asymmetric steering via interference effects induced by closed-loop coupling, Phys. Rev. A **99**, 022335 (2019).

[53] S. Y. Guan, H. F. Wang, and X. X. Yi, Cooperative-effect-induced one-way steering in open cavity magnonics, npj Quantum Inf. **8**, 102 (2022).

[54] N. Wang, Z. B. Yang, S. Y. Li, T. T. Dong, and A. D. Zhu, Parametric controllable one-way quantum steering induced by four-wave mixing in cavity magnonics, EPJ Quantum Technol. **10**, 15 (2023).

[55] S. V. Kutsaev, A. Krasnok, S. N. Romanenko, A. Y. Smirnov, K. Taletski, and V. P. Yakovlev, Up-and-coming advances in optical and microwave nonreciprocity: From classical to quantum realm, Adv. Photon. Res. **2**, 2000104 (2021).

[56] L. Tang, J. Tang, M. Chen, F. Nori, M. Xiao, and K. Xia, Quantum squeezing induced optical nonreciprocity, Phys. Rev. Lett. **128**, 083604 (2022).

[57] C. P. Shen, J. Q. Chen, X. F. Pan, Y. M. Ren, X. L. Dong, X. L. Hei, Y. F. Qiao, and P. B. Li, Tunable nonreciprocal photon correlations induced by directional quantum squeezing, Phys. Rev. A **108**, 023716 (2023).

[58] S. Liu, Y. Lou, Y. Chen, and J. Jing, All-optical entanglement swapping, Phys. Rev. Lett. **128**, 060503 (2022).

[59] A. B. Matsko and V. S. Ilchenko, Optical resonators with whispering-gallery modes—Part I: Basics, IEEE J. Sel. Top. Quantum Electron. **12**, 3 (2006).

[60] V. S. Ilchenko and A. B. Matsko, Optical resonators with whispering-gallery modes—Part II: Applications, IEEE J. Sel. Top. Quantum Electron. **12**, 15 (2006).

[61] S. Yang, Y. Wang, and H. Sun, Advances and prospects for whispering gallery mode microcavities, Adv. Opt. Mater. **3**, 1136 (2015).

[62] D. Y. Wang, L. L. Yan, S. L. Su, C. H. Bai, H. F. Wang, and E. Liang, Squeezing-induced nonreciprocal photon blockade in an optomechanical microresonator, Opt. Express **31**, 22343 (2023).

[63] G. Vidal and R. F. Werner, Computable measure of entanglement, Phys. Rev. A **65**, 032314 (2002).